

Digital Clay: Kinematic Mechanism Designs and Computational Issues for Haptic Shape Display

Paul Bosscher, *Member, IEEE*, and Imme Ebert-Uphoff, *Member, IEEE*

Abstract—This paper examines the kinematic design of Digital Clay, a new type of computer interface that creates physical 3D shapes that a user can interact with. After enumerating the design specifications for the Digital Clay, a new set of kinematic architectures is introduced: the Formable Crust Mechanisms. These formable crust mechanisms can form shapes in much the same way a piece of fabric would and have tremendous potential for shape generation. Two measures, the Surface Freedom Measure and the Freedom from Ground Measure, are introduced to aid in evaluating potential designs. The various architectures are evaluated and compared leading to the selection of the most promising mechanisms. Lastly, issues regarding computation of kinematic equations and mechanism pose optimization are addressed.

Index Terms—haptics, shape display, digital clay, mechanism design

I. INTRODUCTION

The Digital Clay Project is an NSF-sponsored research project at the Georgia Institute of Technology. Its objective is the research and design of a new type of computer interface known as ‘Digital Clay,’ a desktop device designed to form into a variety of shapes. Digital Clay will provide a user with a tactile interaction with the virtual world, generating three-dimensional surfaces via an actuated kinematic structure, such as the one in Figure 1. It will be both an input and output device, formed either by a user physically manipulating the surface of the clay or by computer controlled actuation of fluidic actuators embedded within the structure.

The technology that is used to build this device will be entirely scalable, including MEMS and rapid prototyping technologies. Thus, as MEMS and rapid prototyping technologies improve, the device can be scaled down, improving the spatial resolution of the resulting surface.

The potential benefits of this device could be far reaching. Digital Clay would not only allow users a richer interaction with a 3D virtual world, it could also be used to provide engineers with instant 3D prototypes of CAD models and allow them to manipulate those CAD models in a very simple and intuitive manner. Digital Clay also has the potential to improve the ease with which the visually impaired use computers.

The research described in this article is part of a multi-disciplinary effort [1] to make Digital Clay a reality. While

P. Bosscher is a student in the mechanical engineering department at the Georgia Institute of Technology, Atlanta GA 30332 (e-mail: gtg299d@mail.gatech.edu)

I. Ebert-Uphoff is an assistant professor with the mechanical engineering department at the Georgia Institute of Technology, Atlanta, GA 30332 (e-mail: ebert@me.gatech.edu)

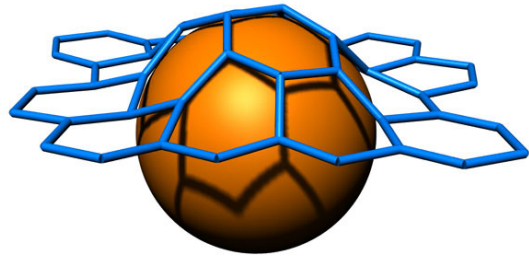


Fig. 1. Formable Crust Mechanism Forming to a Sphere.

other research groups at Georgia Tech, namely the research groups of Dr. Wayne Book (ME), Dr. David Rosen (ME), Dr. Mark Allen (ECE), Dr. Ari Glezer (ME), Dr. Jarek Rossignac (CS) and Dr. Chris Shaw (CS), focus on the manufacturing, control [2] and human interface aspects [3] of Digital Clay, the authors’ focus is to select kinematic architectures for Digital Clay.

This article describes work related to digital clay (Sect. II), specifications for the design (Sect. III), potential architecture designs (Sect. IV) and evaluation measures (Sect. V). These measures are used to compare the designs (Sect. VI), leading to selection of the most promising mechanism designs. Some computational issues relating to the utilization of these mechanisms are discussed (Sect. VII), followed by a brief discussion of future work (Sect. VIII).

II. RELATED WORK

Currently, interacting with virtual 3-D objects is not typically done via a physical representation of the objects. The predominant method of creating and manipulating virtual objects is with CAD programs such as ProEngineer, AutoCAD, IDEAS, SDRC, SolidWorks, etc.¹

A more natural method of creating and manipulating virtual objects was developed in the form of glove-based input, where editing of virtual objects can be performed by computerized interpretation of a user’s hand motions. Many of these gloves do not provide tactile interaction with the objects and thus do not improve the user’s perception of the object.

In order to augment the capacity of glove-based interaction with virtual objects, some researchers have added mechanisms to glove-based systems in order to provide haptic feedback for the user, such as the CyberGrasp [4] and the RM-II Hand Master [5], both of which are shown in Figure 2. Many of

¹All CAD software trade names are copyright of their respective owners



Fig. 2. The CyberGrasp [4] (left) and RM-II Hand Master [5] (right).

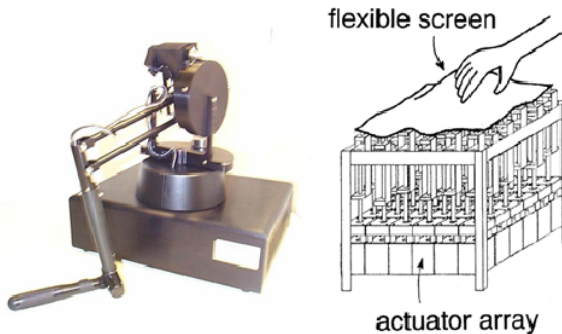


Fig. 3. The PHANTOM [8] (left) and FEELEX [7] (right).

the various glove-based input devices are summarized in [6]. However, some researchers, such as Iwata [7], criticize such devices as being cumbersome and impractical.

An alternative to glove-based interaction is to use devices that provide point-contact interaction with virtual objects via a pen-like interface. Such devices include the well-known PHANTOM [8], shown on the left in Figure 3 and a similar device by Iwata [7]. These point-contact devices were studied by Kirkpatrick and Douglas [9] and were evaluated in how effectively they conveyed the shape of a virtual object to a user. Based on human trials they concluded that, “This class of devices does not appear to support adequate performance for applications that require geometric perception.”

Another method for communicating shape is to create a device that can physically represent a shape. Thus far there have been very few attempts to create shapes for haptic display using mechanisms. Furthermore, nearly all of the research on creating shapes with mechanisms has been based on ‘bed-of-nails’ mechanisms. These mechanisms use an array of closely packed nails or pins that can be raised in order to form the desired surface. Such mechanisms include the FEELEX [10], the Tactile Shape Display [11], and the ItactI [12]. The FEELEX is shown on the right in Figure 3 and is representative of the general construction of such devices.

III. DESIGN SPECIFICATIONS

Given the desired functionality of Digital Clay, the kinematic structure of the device is designed to meet several different specifications:

1. Ability to Form Shapes - This criterion is possibly the most important. The structure should be able to accurately represent a large variety of shapes.

2. Kinematically Determined - The Digital Clay should be *exactly* kinematically determined, so that when all actuators are fixed, the surface is fixed but the structure is not over-constrained.

3. Straightforward Kinematics - The kinematic equations should be simple, thus allowing for faster calculation of the forward and inverse kinematics. Because Digital Clay will eventually incorporate a very large number of actuators, it is important to keep the computational demands low so that the software controlling the device can function at a reasonable speed.

4. Mechanical Strength and Rigidity - The mechanical strength and rigidity of the structure is important for several reasons. First, the structure must be strong enough to withstand manipulation by external forces and actuator forces. Second, it must maintain rigidity when the actuators are fixed. External forces applied to the structure should not cause significant deformation if the actuators are locked.

5. High Resolution - There are three types of resolution that are important. *Spatial resolution* describes how small an area of the surface can be manipulated, and is expressed in terms of the number of surface points per unit area. Surface points will be discussed in detail in Section V-A.1. *Data resolution* is the ratio of the degrees of freedom of the surface to the total number of actuators and is discussed in detail in Section V-C. *Displacement resolution* is a measure of how finely the position of the surface can be controlled.

6. Manufacturability - This specification is particularly important because every part of the device must be built using scalable manufacturing techniques. This places limitations on the types of joints and actuators available for use in the design. These limitations, as well as the limitations on the scale of the structure, depend on the manufacturing technology available. Research on the manufacturing of the architectures presented in this article is carried out by two other research groups at Georgia Tech, namely Dr. Rosen’s group addresses the Rapid Prototyping aspects and Dr. Allen’s group develops customized actuators using MEMS technology. While that research is by far beyond the scope of this paper, the manufacturing aspects were taken into account for the development of the architectures presented here.

IV. FORMABLE CRUST DESIGNS

A new set of mechanism architectures, named *Formable Crust Mechanisms*, shows a great deal of promise for generating a wide variety of shapes. The idea behind these formable crusts is to build a grid-like structure that can form surfaces in a way similar to fabric or a sheet of rubber. The crusts will have a repetitive structured pattern, allowing for straightforward propagation of the forward kinematics and producing structures that are suitable for mass-fabrication by scalable methods. These formable crusts are made possible by the use of the Spherical Joint Mechanism (SJM), a joint mechanism that allows multiple links to be connected to a single spherical joint. A prototype version of the SJM is shown in Figure 4. The darkened links are main links which are connected to each other via revolute joints and

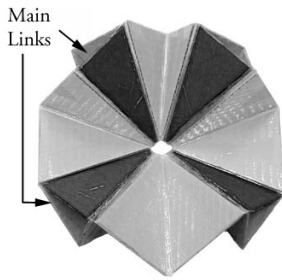


Fig. 4. Prototype of Spherical Joint Mechanism.

two intermediate links. The axes of all of the revolute joints intersect at a single point in the center of the mechanism, producing spherical connections between the main links. The SJM is discussed in detail in [13].

This section will present some of the crust architectures. This is not an exhaustive list of possible designs, but a brief introduction to formable crust mechanisms. The crusts presented here will be evaluated in detail in section VI.

A. First Generation Designs

The first generation of formable crust designs consists of two designs, described in sections IV-A.1 and IV-A.2. These two designs use only spherical joints, which are constructed using the SJM. Every link represents an element of the surface.

1) *Square Grid Crust:* The Square Grid Crust is diagrammed in Figure 5. It consists of a regular pattern of square ‘cells’ with every link attached to other links in the mechanism by spherical joints. The regular pattern of cells of this crust (and all other crusts) can be repeated to produce as large a crust as necessary. As is clearly shown in the diagram, every spherical joint connects four links together with collocated spherical connections.

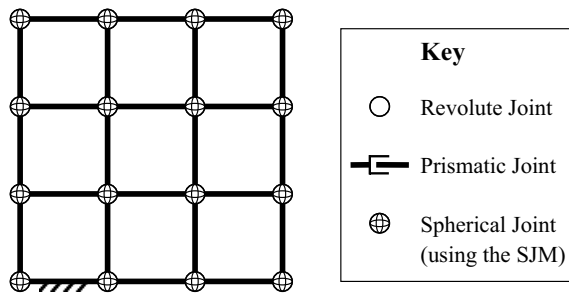


Fig. 5. Diagram of Square Grid Crust.

2) *Hex Grid Crust:* The Hex Grid Crust, diagrammed in Figure 6, consists of a regular pattern of hexagonal cells.

Figure 1 illustrates how a formable crust mechanism can deform to represent a desired shape. This figure illustrates a Hex Grid Crust lowered onto a sphere and taking the shape of the sphere. A user feeling the top of the crust would be able to feel the representation of the top portion of the sphere. This figure also illustrates how the crust would respond to deformation by the user, as the sphere could represent a user’s finger pressing into the crust.

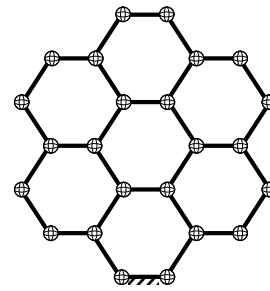


Fig. 6. Diagram of Hex Grid Crust.

B. Second Generation Designs

While prototypes of the first generation of crust designs proved to be very formable, they also exhibited a high degree of coupling between their links. That is, displacement of one portion of the crust resulted in displacement of nearly every link in the crust. If deformation of the crust could be localized, displacement of a portion of the crust could occur with the use of only a few actuators, rather than requiring the use of nearly all of the actuators. Localized deformation of the crust requires that the crust behave less like a piece of fabric and more like a sheet of rubber. The ability to ‘stretch’ the crust can be made possible by incorporating prismatic joints into the crust. The following designs incorporate both passive and actuated revolute and prismatic joints.

1) *Square Grid Crust with Prismatic Joints:* The Square Grid Crust with Prismatic Joints (Fig.7) is a simple modification of the Square Grid Crust. The addition of prismatic joints allows for the distances between neighboring spherical joints to be varied, which greatly increases the formability of the crust and allows for localized deformation.

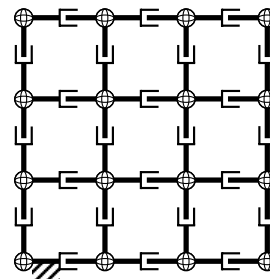


Fig. 7. Diagram of Square Grid Crust with Prismatic Joints. (For key see Fig. 5)

2) *Hex Grid Crust with Prismatic Joints:* The Hex Grid Crust with Prismatic Joints, shown in Figure 8, is a simple modification of the Hex Grid Crust. The addition of prismatic joints greatly increases the formability of the crust.

C. Third Generation Designs

The second generation designs of formable crusts had a significantly improved ability to form shapes. However, experiments in rapid prototyping and similar technology indicate that prismatic joints (both passive and actuated) may be very difficult to manufacture using scalable methods. Accordingly, the third generation designs are intended to achieve the same

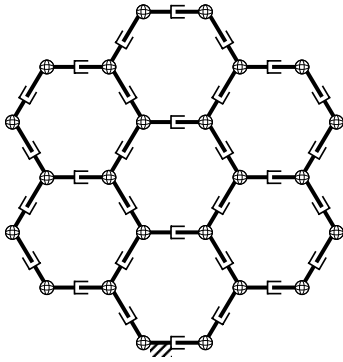


Fig. 8. Diagram of Hex Grid Crust with Prismatic Joints. (For key see Fig. 5)

functionality as the second generation designs, but only using revolute joints.

1) *Hinged Square Grid Crust*: The Hinged Square Grid Crust, diagrammed in Figure 9, is similar to the Square Grid Crust with Prismatic Joints except that the prismatic joints have been replaced by revolute joints. This change still allows for the distance between neighboring spherical joints to be varied, but differs significantly in the representation of the surface. Previously the surface was represented by all of a crust's links. Now, the surface is represented by just the crust's spherical joints. That is, each of the spherical joints within the hinged square grid crust represents a distinct point on the surface. This is illustrated in Figure 10, which shows a simple model of the Hinged Square Grid Crust. Each of the raised spheres in the model represents a spherical joint of the crust. Each of these raised spheres, therefore, represents a point on the surface.

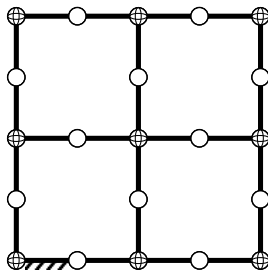


Fig. 9. Diagram of Hinged Square Grid Crust. (For key see Fig. 5)

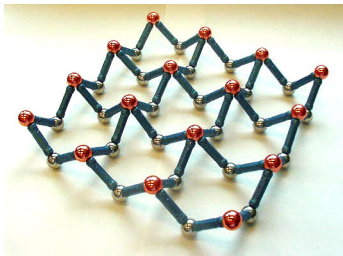


Fig. 10. Model of Hinged Square Grid - Oblique View.

2) *Alternate Hex Grid Crust*: The topological structure of the Alternate Hex Grid Crust, shown in Figure 11, is identical

to that of the Hex Grid Crust (Fig. 6). The difference between them is that while the Hex Grid Crust represents the surface with the links, the Alternate Hex Grid Crust represents the surface with every other spherical joint. Figure 11 shows clearly how every other spherical joint is raised. Each of these raised joints represents a point on the surface.

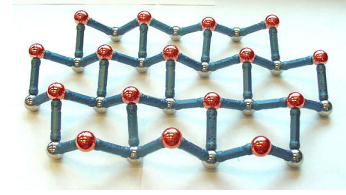


Fig. 11. Model of Alternate Hex Grid Crust - Oblique View.

D. Actuator Placement

The repetitive structure of the crust mechanisms makes it relatively easy to develop schemes for actuator placement. Because each crust can be subdivided into 'cells' (square, hexagonal, etc.) it is possible to establish actuator arrangements that actuate a single cell. The actuation of the cells can then be propagated through the crust until the entire mechanism is actuated using the following procedure: 1) Start with a cell that is fixed to the ground. Choose the placement of actuators such that every link in the cell is exactly determined. Note that if the cell is exactly determined by the actuators there will be as many actuators as degrees of freedom of the cell. 2) Select a cell adjacent to the fixed cell. Choose placement of actuators such that this cell is exactly determined. 3) Repeat this procedure, propagating outwards from the first cell until the entire structure is actuated.

This method not only simplifies the process of selecting actuator locations, it also results in simplified forward kinematics with a recursive form. The computational issues associated with the kinematic equations will be discussed in Section VII and a more complete discussion of actuation propagation can be found in [14].

V. MEASURES

As stated in Section III, the most important characteristic of the Digital Clay is its ability to form shapes. The ability of a structure to form shapes depends on the relative freedom between the elements that define the surface and the range of motion of the structure. Two measures, the Surface Freedom Measure and the Freedom from Ground Measure are presented here to aid in evaluating the ability of potential structures to form shapes.

A. Surface Freedom Measure

Because the shapes made by the Clay are defined by a set of elements that represent a surface, the ability to form shapes depends on the potential for these elements to move freely and independently through a large range of motion. The first performance measure for the structure is the Surface Freedom Measure (SFM).

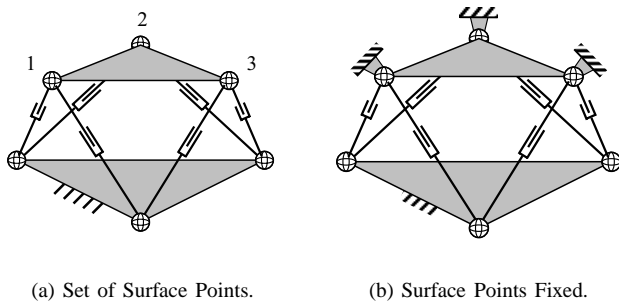


Fig. 12. Example Mechanism - The 3-3 Gough Stewart Platform

1) *Surface Points*: Given that certain elements of a mechanism are chosen to represent a surface, it is of interest to assign *surface points* to these *surface elements*. Surface elements are the parts of the structure that represent the surface and are manipulated by the user. Surface points are points that are attached to the surface elements and are used to describe the positions and orientations of the surface elements. A set of surface points is an *allowable set* if and only if the positions of the surface points completely define the positions and orientations of the surface elements. That is, if the positions of the surface points are known then the positions and orientations of the surface elements are known completely. A *minimal set* of surface points is an allowable set of surface points with the least number of points necessary. Note that no surface points are associated with the ground.

An example of choosing surface points for a mechanism is shown in Figure 12(a). This mechanism is a 3-3 Gough-Stewart platform. The upper platform is considered to be the only surface element and because it is a planar element the minimal set of surface points will consist of three points. A convenient choice of surface points is the set of points that coincide with the centers of joints 1, 2 and 3 as labeled in the figure.

2) *Calculating the Surface Freedom Measure*: The Surface Freedom Measure is defined as:

$$SFM = \frac{(F - E)}{n} \quad (1)$$

where F is the number of degrees of freedom of the mechanism, E is the number of extraneous degrees of freedom of the mechanism, and n is the number of surface points. In many cases F may be determined using Grübler's mobility formula [15]:

$$F = \lambda(\ell - j - 1) + \sum_{i=1}^j f_i \quad (2)$$

where λ is the motion parameter (3 for a planar or spherical mechanism, 6 for a spatial mechanism), ℓ is the number of links in the mechanism including the ground, j is the number of joints in the mechanism, assuming that all joints are binary, and f_i is the degrees of relative freedom permitted by joint i . However, in some cases Grübler's equation does not apply due to the geometric structure of the mechanism. A solution to this problem is discussed in [16].

E , the number of *extraneous degrees of freedom*, represents the degrees of freedom of the mechanism that do not produce any motion of the surface points. In order to determine the extraneous degrees of freedom of more complicated mechanisms each of the surface points may be fixed in space by attaching a virtual spherical joint between each surface point and the ground. Any remaining degrees of freedom of the mechanism will be E , the extraneous degrees of freedom. Figure 12(b) illustrates how to determine the extraneous degrees of freedom of the 3-3 Gough-Stewart platform shown previously in Figure 12(a). Using the surface points chosen previously that coincide with joints 1, 2 and 3, the surface points may be fixed in space by rigidly attaching each of these three joints to the ground as illustrated. Analysis of this altered structure reveals that there are six remaining degrees of freedom - the rotation of each leg about the axis passing through the two spherical joints at each of its ends; thus E is 6.

3) *Interpreting the Surface Freedom Measure*: The SFM of a mechanism is the ratio of the number of degrees of freedom of the surface to the number of surface points, resulting in a measure of the average number of degrees of freedom per surface point. Thus, a high SFM indicates a better ability to form shapes. If a minimal set of surface points is used the lowest possible SFM of a structure is 1 and the highest possible SFM of a structure is 3. The SFM describes the ability of the structure to move surface points independently, and thus is a strong indicator of the structure's ability to create shapes effectively.

The SFM does not give any information on the range of motion of the structure. As the SFM is only a function of the topology of the structure it does not take into account many of the factors that determine the range of motion of the structure, such as actuator placement, actuator limits and kinematic parameters.

B. Freedom from Ground Measure

As was mentioned in the previous section, the Surface Freedom Measure does not give any information on the range of motion of a structure. The Freedom from Ground Measure (FGM) is a measure that provides an indication of the range of motion of a structure based on its topology.

1) *Path Lengths*: The ability of a surface to form shapes also depends on the ability of surface points to move a significant distance; i.e. to have a large range of motion. Without knowing the kinematic parameters of a structure it is of course impossible to know the exact range of motion of each surface point. However, it is possible to analyze the degree to which a surface point is constrained by connection to the ground.

In order to describe the degree to which surface points are limited in range of motion by connection to the ground, it is necessary to determine the *path length* between points on a mechanism. By analyzing the graph of a mechanism, a straightforward definition of the path length between two points may be established.

A graph is composed of a set of vertices and a set of edges or lines that are connected to these vertices. The graph

representation of a mechanism uses vertices to represent links and lines to represent kinematic pairs. Thus, the graph of a mechanism may easily be formed by replacing each link with a vertex and connecting these vertices with the appropriate lines to represent the joints. Graph representation of mechanisms is discussed in greater detail in [15].

Given the graph of a mechanism, it is now of interest to examine walks and paths within the mechanism. A *walk* is defined as a sequence of alternating vertices and edges starting with a vertex and ending with a vertex. If all of the vertices and edges in the walk are distinct it is called a *path*.

It is also useful to define the *weighted* path length. The weighted length of a path factors in the number of joint freedoms represented by each edge. The weighted path length of a path with m edges is defined as:

$$\text{WeightedPathLength} = \sum_{i=1}^m f_i \quad (3)$$

where f_i is the number of freedoms of the joint represented by edge i in the path. Note that this is equivalent to replacing multi-DOF joints with an equivalent set of links and single-DOF joints.

2) *Calculating the Freedom from Ground Measure:* The Freedom from Ground Measure is a measure that evaluates the potential for a mechanism to produce a large range of motion of surface points based on weighted path lengths within the mechanism. The FGM is the minimum weighted path length from the ground to each surface point averaged over all of the surface points, factoring out passive degrees of freedom.

The Freedom from Ground Measure is defined as:

$$\text{FGM} = \frac{\sum_{i=1}^n \left(\min_{k=1}^{K_i} \left(\sum_{j=1}^m f_j - P_k \right) \right)}{n} \quad (4)$$

where there are n surface points, and surface point i has K_i different paths from the surface point to the ground. Each path k contains m edges (joints). f_j is the number of joint freedoms of joint j in path k , while P_k is the number of passive degrees of freedom in path k . A passive degree of freedom occurs when a link is connected to exactly two other links and may freely rotate about a line connecting the two joints without transmitting any torque.

A sample mechanism is shown in Figure 13(a) and all joints (a) - (i) are spherical. Surface points can be chosen to coincide with the centers of all of the spherical joints except for joints a and b because they are fixed to the ground. Note that in this case the surface points need not be associated with any particular links. Because the surface points are at the centers of the spherical joints they may be considered to be attached to any of the links that attach to that joint with equal validity. That is, the surface point located at the center of joint g can be considered to be attached to either link 8 or link 11 or both.

The graph of the mechanism in Figure 13(a) is shown in Figure 13(b). Note that node 1 is a double circle indicating that it is the link fixed to the ground. It is important to note that every spherical joint connecting three or more links together is represented by more than one edge in the graph. For example,

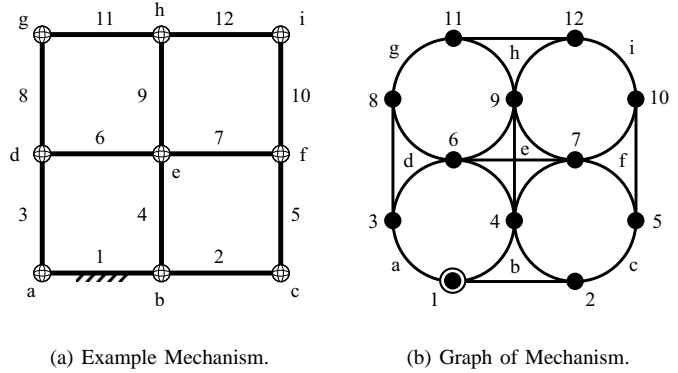


Fig. 13. Path Length Example Mechanism.

joint h connects links 9, 11 and 12 together. Because each link has a spherical connection to the other two the joint is represented by three edges. In order to determine the FGM of this mechanism it is important to clarify how the paths within the mechanism are chosen. Because each surface point is located at the center of a spherical joint, each of these surface points can be considered to be a part of each of the links that is attached to this joint. Thus, when weighted path lengths are calculated to a surface point, paths to *all* possible links associated with that surface point must be included. The FGM for this mechanism is $24/7$, or approximately 3.429.

3) *Interpreting the Freedom from Ground Measure:* The FGM is a measure of the average distance that a surface point is from the ground in terms of joint freedoms. The lowest possible FGM is 1, but there is no upper bound to the FGM. The larger the FGM, the less the surface points are constrained by connection to the ground and the more likely it is that the surface points will have a large range of motion, thus a larger FGM is better. However, it is also important to note that structures with high FGMs may, in some cases, have difficulty maintaining rigidity. The lack of connection to the ground provides greater freedom of motion, but also lessens the mechanical support of the structure. Modifications of crust designs have been developed that provide additional support, but due to space limitations they will not be presented in this paper. Note that this measure is only an indication of the degree to which a mechanism is or is not constrained by the ground. Without knowing the actual kinematic parameters of any given mechanism it is impossible to determine its physical range of motion.

C. Data Resolution

As mentioned in Section III, the Data Resolution (DR) of a structure is the ratio of the information that is represented by the surface to the number of actuators. The DR describes the structure's efficiency at translating information put into the structure (actuator positions) into information displayed by the surface of the structure (surface position) and is calculated by:

$$\text{DR} = \frac{(F - E)}{A} \quad (5)$$

Mechanism	Fig. #	n	F	E	Measures					
					as drawn			limit (as $n \rightarrow \infty$)		
					DR	SFM	FGM	DR	SFM	FGM
Best Possible Value	-	-	-	-	1	3	∞	1	3	∞
FEELEX	2	36	36	0	1	1	1	1	1	1
Square Grid Crust	4	14	42	24	0.43	1.29	5.14	0.33	1	∞
Hex Grid Crust	5	22	66	29	0.56	1.68	7.45	0.5	1.5	∞
Square Grid Crust with Prismatic Actuators	6	14	65	23	0.65	3	7.71	0.5	3	∞
Hex Grid Crust with Prismatic Actuators	7	22	95	29	0.69	3	11.18	0.67	3	∞
Hinged Square Grid Crust	8	8	33	11	0.67	2.75	5.25	0.6	3	∞
Alternate Hex Grid Crust	5,10	11	66	34	0.48	2.91	7.45	0.5	3	∞

TABLE I
COMPARISON OF VARIOUS SHAPE GENERATING MECHANISMS.

where F is the degrees of freedom of the structure, E is the number of extraneous degrees of freedom, and A is the number of actuators where each actuator has a single degree of freedom. F and E can be found in the manner described in Section V-A.2. The data resolution of a structure may range from 0 to 1, with 1 being the best possible resolution.

VI. EVALUATION

The crusts previously presented and the FEELEX (Fig. 3) are evaluated in Table I. The parameters n , F and E are given for the mechanisms as they are diagrammed in the listed figures. The Data Resolution (DR), Surface Freedom Measure (SFM) and Freedom from Ground Measure (FGM) are given for the structures as they are drawn in the figures. The values of the measures are also given for the case where the number of surface points is increased towards infinity.² It is important to note that because the final implementations of the Digital Clay will have a very large number of cells, it is appropriate to compare designs based only on the limiting values of the measures as the structures are expanded.

When evaluating the various designs the most important criterion is the ability to form shapes, which is indicated by the SFM and FGM. As the FGM of every crust design increases as the crusts are expanded, it is likely that all of these designs will have sufficient range of motion. In contrast, the FEELEX is the only structure limited to an FGM of 1, highlighting its limited ability to form shapes that differ significantly from planar shapes.

Further examination of the data in Table I shows that the second and third generation designs have the best SFMs, each with a limiting value of 3. The DRs of these four designs range from 0.5 to 0.667, all of which are acceptable.

Although there are no measures of manufacturability, it is likely that building revolute joints only will be easier than building revolute and prismatic joints. Thus, due to their high SFMs, good DRs and use of only revolute joints, the Hinged Square Grid Crust and the Alternate Hex Grid Crust appear

²Because it is assumed that n is a minimal set of surface points, $n \rightarrow \infty$ implies that for crust mechanisms the number of cells approaches ∞ .

to be the best candidates for the Digital Clay out of the architectures considered thus far.

VII. IMPLEMENTATION AND COMPUTATIONAL ISSUES

Thus far it has been established that formable crust mechanisms are well suited for shape representation. However, some issues remain as to how these mechanisms must be used in order to function as an interactive haptic shape display.

Figure 14 illustrates the process of using a formable crust mechanism for shape display. The sequence of steps along the top of the flowchart describe the computations performed in output mode, where the shape of the Digital Clay is controlled by a computer to represent a desired shape. The 'Surface Point Placement' block takes a mathematical model of the desired surface and selects optimal locations of the surface points and thus specifies the mechanism pose. Surface point placement will be discussed in Section VII-C. Note that in addition to the surface point locations the extraneous degrees of freedom must be specified. Due to space limitations this will not be discussed here but can be found in [14]. The 'Inverse Kinematic Equations' block represents the equations that take a particular pose of the mechanism and produce the corresponding actuator lengths/angles for that pose. The inverse kinematics will be discussed in Section VII-A. Note that in order to formulate the forward or inverse kinematic equations, it is necessary to first select the locations of the actuators within the mechanism as was described in Section IV-D.

The sequence of steps along the bottom of the flowchart describe the computations performed in input mode, where the user manually deforms the Digital Clay and the resulting surface must be read into the computer. The 'Forward Kinematic Equations' block represents the equations that, given the current lengths/angles of the actuators, produce the corresponding pose of the mechanism in terms of the locations of the surface points in space. The forward kinematics will be discussed in Section VII-B. The 'Surface Modeling' block represents the conversion of the positions of the discrete surface points into a mathematical model of the resulting

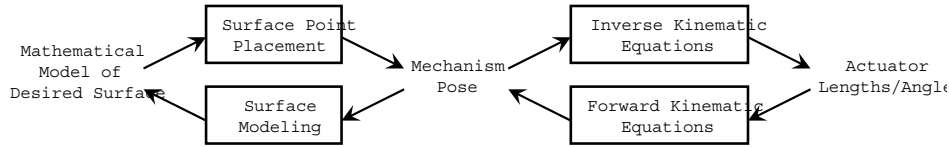


Fig. 14. Flowchart of Steps for Crust Mechanism Utilization.

surface. This modeling may be done through a variety of methods but will not be discussed here.

A. Inverse Kinematics

The inverse kinematics of nearly all formable crust designs reduce to the formation of the inverse kinematics of the SJM, which are described in detail in [14]. The process of calculating the inverse kinematics is scalable. That is, the number of computations that must be performed are proportional to the number of cells in the mechanism. In addition, the inverse kinematic equations are relatively straightforward and not computationally intensive.

B. Forward Kinematics

The forward kinematics of the Formable Crust Mechanisms are more complicated than the inverse kinematics, as is typically the case for mechanisms with closed kinematic chains. However, the forward kinematics can be solved for with reasonable effort because of the repetitive structure of the mechanism and the way the actuation scheme was chosen. By propagating of the forward kinematics outwards from the cell fixed to the ground in the same order as the actuation propagation, the kinematics of each cell becomes decoupled. Thus correct propagation of the kinematic equations reduces the forward kinematics of a *very* large coupled mechanism to the forward kinematics of single cells. As a result, the number of computations required by the forward kinematics are proportional to the number of cells in the crust (for more details, see [14]).

C. Surface Point Placement

To represent a surface, the desired pose of the mechanism must first be determined before the inverse kinematics can be applied. Because a crust mechanism represents a surface by the locations of the surface points of the crust mechanism, each of these points on the mechanism must lie on the desired surface. However, there is still freedom to choose where these surface points lie on the surface. Several simple methods for projecting the surface points onto the desired surface may be possible. For example, if the surface can be described as $z = f(x, y)$ in an x - y - z coordinate frame, the grid of the crust can be placed in the x - y plane and projected in the z direction onto the desired surface. However, such a projection does not guarantee that the resulting locations of the surface points can be ‘reached’ by the crust mechanism.

The primary goal considered here is to choose the locations of these surface points such that these points can be reached by the crust mechanism. That is, it must be possible to place

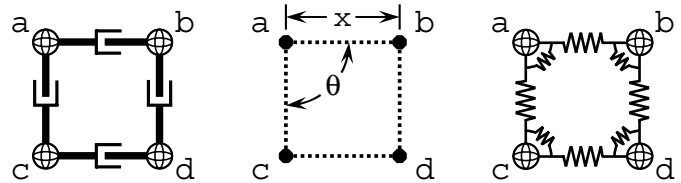


Fig. 15. Diagram of a cell of the Square Grid Crust with Prismatic Joints (left), its relative motion model (center) and the corresponding spring mesh (right).

the surface points of the mechanism at these desired locations without violating any mechanism constraints or any joint limits. The ideal placement of these surface points would not only be reachable, but would also keep most (or all) of the joints within the mechanism near the middle of their range of motion. This would result in maximizing the amount of change of shape that the crust could undergo from this original pose.

A method for placing the surface points effectively, termed the ‘spring mesh’ method, has been developed and will be described in this section. This method of surface point placement is based on two assumptions. First, it is assumed that individual points are being placed on the surface, rather than linear or planar elements. Second, it is assumed that every surface point can be placed independently of all other surface points. This is the case for every mechanism that has a Surface Freedom Measure that approaches 3 as more cells are added to the mechanism. These assumptions are valid for nearly all of the more promising crust designs.

1) *Spring Mesh Method*: The spring mesh method of surface point placement is based on a simplified model of the relative range of motion of surface points. This model approximates the relative range of motion of surface points with relative angle and displacement limits. To better illustrate this concept, Figure 15 diagrams a single cell of the Square Grid Crust with Prismatic Joints. The surface points of this cell are points a , b , c and d . If we now only consider those points, we can construct line segments joining adjacent surface points, as illustrated at the center of Figure 15. The model for the relative range of motion of surface points is that the distance between adjacent surface points and the angle between adjacent line segments can vary about a nominal distance and angle, respectively. That is, the distance x between points a and b can vary about some nominal distance x_0 by $\pm\Delta x$ and the angle θ between line segments a - b and a - c can vary about some nominal angle θ_0 by $\pm\Delta\theta$. While the true range of motion of surface points is not this decoupled, this approximation is reasonably valid. Discussion of the limitations of this method can be found in [14].

An ideal set of surface points can now be described as the

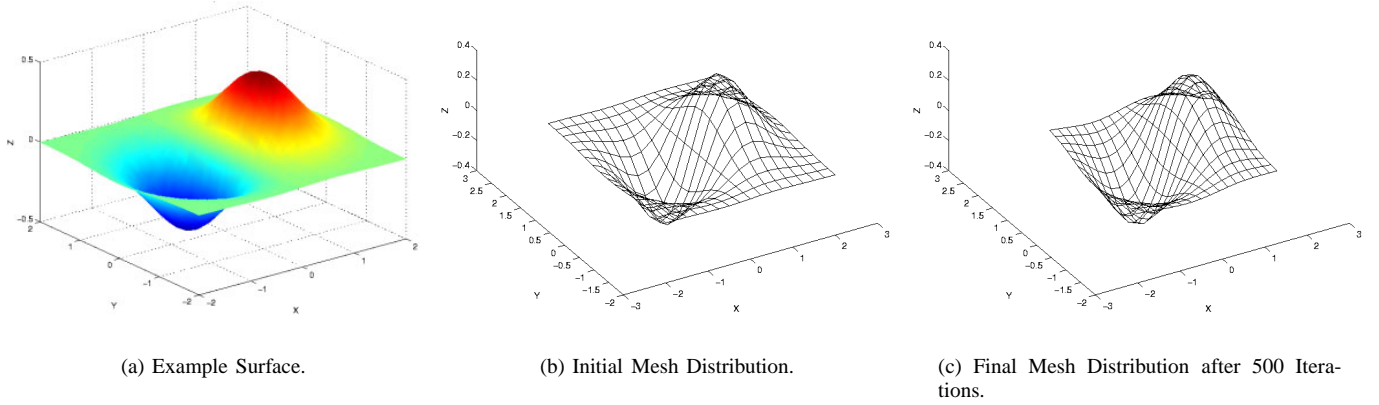


Fig. 16. Example Mesh Optimization

set of points that minimizes the deviation of each x and θ from its nominal displacement x_0 and θ_0 , respectively. The range of motion of the crust may be modeled by converting the set of surface points and linear segments into a mesh of springs. This spring mesh is created by replacing every line segment in the previous illustration with a linear spring and adding an angular spring between all adjacent line segments. This construction of a spring mesh is illustrated on the right in Figure 15. An optimized set of surface points can now be found by constraining the surface points of the mesh to lie on the desired surface and minimizing the total potential stored in all of the springs. This minimization will result in a set of surface points where the entire spring mesh is in static equilibrium, with each spring acting to keep each linear and angular joint as close as possible to its nominal length or angle.

If each line segment is assigned a linear stiffness $k_{lin,i}$ and each angle between line segments is given an angular stiffness $k_{ang,j}$ and all springs are linear (versus non-linear) and if a given set of surface point positions is given by the vector \mathbf{P} , then the optimal set of surface point positions \mathbf{P}_{des} satisfies the following:

$$F(\mathbf{P}_{des}) = \min_{\mathbf{P} \in Q} F(\mathbf{P}) \quad (6)$$

$$Q = \{\mathbf{P} \mid G(\mathbf{P}) = 0\} \quad (7)$$

where the constraint that all the surface points in \mathbf{P} must lie on the desired surface can be expressed as $G(\mathbf{P}) = 0$ and F is the potential energy stored in the spring mesh,

$$F = \frac{1}{2} \sum_{i=1}^m k_{lin,i} (x_i - x_{i,0})^2 + \frac{1}{2} \sum_{j=1}^n k_{ang,j} (\theta_j - \theta_{j,0})^2 \quad (8)$$

where there are m line segments and n angles between adjacent line segments.

2) *Implementation*: Given the spring mesh described in the previous section, the next step is to minimize F subject to the constraint that all surface points must lie on the desired surface. One possible minimization technique is using a global method, in which a single simultaneous optimization of all of the surface points is performed. Because of the large number of surface points in a crust mechanism, formulating such an

optimization would be very complex and would require a large amount of computation time. Thus it seems appropriate to use a simpler method to implement this minimization.

The minimization used here is a simple iterative method. First, an initial distribution of the surface points is produced by projecting the mesh onto the desired surface. Then, the position of the surface points is optimized one surface point at a time, where all but one of the surface points are held fixed. The position of the surface point that is not held fixed is optimized such that the spring energy stored in the local region of the mesh near the point is minimized. The optimized point is now held fixed and another point is chosen for optimization, and this process continues until every point has been optimized once. This process can now be iterated, with each point being optimized once during the iteration. When iterating this local minimization routine, the energy stored within the springs in the mesh must stay the same or decrease with every step of the iteration. Thus this method is guaranteed to converge to a solution by the Monotone Convergence Theorem [17] and thus is guaranteed to converge to a static equilibrium pose of the spring mesh. A more detailed discussion of this method is included in [14].

3) *Example*: To demonstrate this iterative minimization of F , an example scenario was examined. For this example the crust mechanism used is the Square Grid Crust with Prismatic Joints and the desired surface is:

$$z(x, y) = x \cdot e^{(-x^2 - y^2)} \quad (9)$$

This surface is plotted in Figure 16(a), with all length dimensions assumed to be in meters. The minimization of the total spring energy was performed using MATLAB and the MATLAB simultaneous non-linear equation solver `fsolve`.

For this example all linear springs have a stiffness of $k_{lin} = 10,000$ N/m and all angular springs have a stiffness of $k_{ang} = 500$ N·m/rad. The unstretched length of the linear springs is 0.2 m and the unstretched angle of the angular springs is $\pi/2$. The initial pose of the mesh, shown in Figure 16(b), was generated by forming a square mesh with 0.25 m spacing on the x - y plane and projecting it vertically onto the desired surface. The final distribution that was obtained after 500 iterations is shown in 16(c). A plot of the total

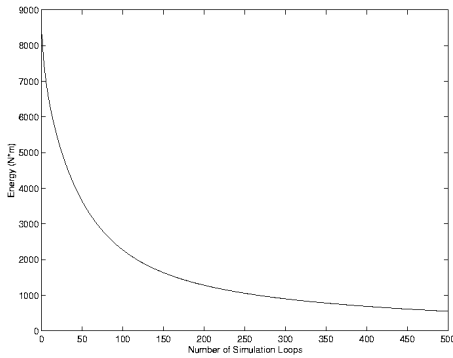


Fig. 17. Mesh Optimization Example - Total Energy Stored in Springs.

potential energy stored in the springs is shown in Figure 17. The roughly exponential decrease of the energy stored in the springs illustrates the convergence of the minimization. Note that in Figures 16(b) and 16(c) each square element in the mesh corresponds to a square cell of the Square Grid Crust with Prismatic Joints, and thus the position of each node of the mesh corresponds to the resulting position of a surface point.

4) *Discussion*: Two key issues arise from this optimization. First, while it has been proven that F will converge and produce a set of surface points corresponding to a mesh in static equilibrium, there is no guarantee that this convergence will happen quickly or that the resulting solution is unique. If there are multiple static equilibrium poses possible for a given mesh and desired surface, there is no way of knowing whether the solution found by this method is the global minimum of F or merely a local minimum of F . In many cases there will not be more than one possible static equilibrium pose, but further studies may need to be performed to address this issue completely.

Second, this approach only produces an ‘optimized’ set of surface points. Whether or not this set of points is possible for the mechanism to reach must still be evaluated using the inverse kinematics. If the points cannot be reached (i.e. there is no solution to the inverse kinematics), some other method of optimization must be employed.

VIII. FUTURE WORK

The work presented in this paper opens up several areas of potential future work:

- 1) *Mechanism Optimization* - Because the scope of this paper was limited to architecture selection and did not address details like link dimensions, the mechanical design of formable crust mechanisms is a significant area of future work.
- 2) *Utilization Optimization* - While an effective method was presented for optimizing the placement of the surface points on the desired surface, there is still a great deal of work that can be done in improving this method. In the spring mesh method only the range of motion of the mechanism is taken into account, but other factors such as singularity avoidance, mechanism rigidity and required actuator forces/torques could also be included.
- 3) *Manufacturing Challenges* - While manufacturing issues

were not directly addressed in this paper, many manufacturing challenges arise from the mechanisms presented here. These challenges include building scalable fluidic actuators, building scalable, flexible tubing to provide fluid to these actuators, and building durable, accurate joints that have sufficient range of motion. Those challenges are currently being addressed by other research groups at Georgia Tech, including efforts to construct a prototype of a formable crust mechanism.

IX. CONCLUSION

This paper has introduced Formable Crust Mechanisms, a new set of mechanism architectures for shape generation. A method of developing actuation schemes for these structures was described. Two measures, the Surface Freedom Measure and the Freedom from Ground Measure, were introduced to aid in the evaluation of these designs. The various architectures were evaluated and compared, leading to the selection of two promising candidate structures for Digital Clay. The forward and inverse kinematics were briefly discussed and a method was proposed for optimizing the placement of the mechanism’s surface points on the desired surface. An example of this optimization was implemented in MATLAB to verify its effectiveness.

ACKNOWLEDGMENT

Support for this work was provided by the National Science Foundation under Grant #IIS-0121663 and by a National Defense Science and Engineering Graduate (NDSEG) Fellowship.

REFERENCES

- [1] J. Rossignac, M. Allen, W. J. Book, A. Glezer, I. Ebert-Uphoff, C. Shaw, D. Rosen, S. Askins, J. Bai, P. Bosscher, J. Gargus, B. Kim, I. Llamas, A. Nguyen, G. Yuan, and H. Zhu, “Finger sculpting with Digital Clay: 3D shape input and output through a computer-controlled real surface,” in *Proceedings of the Shape Modeling International Conference*, Seoul, Korea, May 2003.
- [2] H. Zhu and W. J. Book, “Control concepts for Digital Clay,” in *2003 IFAC Symposium on Robot Control (SyRoCo 2003)*, Wroclaw, Poland, September 2003, accepted.
- [3] I. Llamas, B. Kim, J. Gargus, J. Rossignac, and C. D. Shaw, “Twister: A space-warp operator for the two-handed editing of 3D shapes,” in *Proceedings of the ACM SIGGRAPH*, 2003.
- [4] Immersion Corporation, “<http://www.immersion.com/products/3d/interaction/cybergrasp.shtml>.”
- [5] V. Popescu, G. Burdea, and B. M., “Virtual reality modeling for a haptic glove,” in *Computer Animation 1999*, Geneva, May 1999.
- [6] D. J. Sturman and D. Zeltzer, “A survey of glove-based input,” *IEEE Computer Graphics and Applications*, vol. 14, pp. 30–39, January 1994.
- [7] H. Iwata, “Pen-based haptic virtual environment,” in *Proceedings of the Virtual Reality Annual International Symposium*. Seattle, WA: IEEE, September 1993, pp. 287–292.
- [8] T. H. Massie and J. K. Salisbury, “The PHANTOM haptic interface: A device for probing virtual objects,” in *Proceedings of the ASME Winter Annual Meeting, Symposium on Haptic Interfaces for Virtual Environment and Teleoperator Systems*, Chicago, IL, Nov. 1994.
- [9] A. E. Kirkpatrick and S. A. Douglas, “Application-based evaluation of haptic interfaces,” in *Proceedings of the 10th Symposium on Haptic Interfaces for Virtual Environment and Teleoperator Systems*, Orlando, FL, 2002, pp. 32–39.
- [10] H. Iwata, H. Yano, F. Nakaizumi, and R. Kawamura, “Project FEELEX: Adding haptic surface to graphics,” in *Proceedings of SIGGRAPH2001*, 2001.

- [11] C. R. Wagner, S. J. Lederman, and R. D. Howe, "A tactile shape display using RC servomotors," in *Proceedings of the 10th Symposium on Haptic Interfaces for Virtual Environment and Teleoperator Systems*, Orlando, FL, 2002, pp. 354–355.
- [12] J. Knight and A. Smith, "Interactive tactile interface - ItactI," www.itacti.com, 2001, iST-2001-32240-ITACTI.
- [13] P. Bosscher and I. Ebert-Uphoff, "A novel mechanism for implementing multiple collocated spherical joints," in *Proceedings of the 2003 IEEE International Conference on Robotics and Automation*, 2003.
- [14] P. Bosscher, "Digital clay: Architecture designs for shape-generating mechanisms," Master's thesis, Georgia Institute of Technology, Atlanta, GA, April 2003.
- [15] L.-W. Tsai, *Mechanism Design: Enumeration of Kinematic Structures According to Function*. Boca Raton, FL: CRC Press, 2001.
- [16] W. Kim, S.-E. Lee, and B.-J. Yi, "Mobility analysis of planar mobile robots," in *Proceedings of the 2002 IEEE International Conference on Robotics and Automation*, Washington, DC, 2002, pp. 2861–2867.
- [17] R. G. Bartle, *The Elements of Real Analysis*, 2nd ed. New York: John Wiley & Sons, 1976, ch. 3, pp. 104–105.